

Non-uniform scaling of the magnetic field variations before the M_w 9.0 Tohoku earthquake in 2011

E. S. Skordas^{1,*}

*¹Solid State Section and Solid Earth Physics Institute,
Physics Department, University of Athens,
Panepistimiopolis, Zografos 157 84, Athens, Greece*

Abstract

Applying Detrended Fluctuation Analysis (DFA) to the geomagnetic data recorded at three measuring stations in Japan, Rong et al. in 2012 reported that anomalous magnetic field variations were identified well before the occurrence of the disastrous Tohoku M_w 9.0 earthquake that occurred on 11 March 2011 in Japan exhibiting increased “non-uniform” scaling behavior. Here, we provide an explanation for the appearance of this increase of “non-uniform” scaling on the following grounds: These magnetic field variations are the ones that accompany the electric field variations termed Seismic Electric Signals (SES) activity which have been repeatedly reported that precede major earthquakes. DFA as well as multifractal DFA reveal that the latter electric field variations exhibit scaling behavior as shown by analyzing SES activities observed before major earthquakes in Greece. Hence, when these variations are superimposed on a background of pseudosinusoidal trend, their long range correlation properties -quantified by DFA- are affected resulting in an increase of the “non-uniform” scaling behavior. The same is expected to hold for the former magnetic field variations.

Complex systems exhibit scale invariant features characterized by long-range power-law correlations, which are usually difficult to identify mainly due to the presence of erratic fluctuations and nonstationarity embedded in the emitted signals. For example, the long-range correlation properties of the so called Seismic Electric Signals activities (which are low frequency electric signals of dichotomous nature preceding major earthquakes) are affected by pseudosinusoidal trends. By employing Detrended Fluctuation Analysis (DFA), which has been established as a robust method suitable for detecting long-range power-law correlations embedded in non-stationary signals, it is found that SES activities exhibit infinitely ranged temporal correlations, i.e., with an exponent close to unity. The same holds for the magnetic field variations accompanying SES activities. Recently, the daily scaling properties of geomagnetic field data in the Japanese area have been investigated by DFA for a period more than one year before the occurrence of the devastating Tohoku earthquake of magnitude 9.0 in 2011. Just a few months before its occurrence, an increase of the “non-uniform” scaling behavior was identified. This is explained as follows: In the absence of SES activities, the electrical records exhibit a pseudosinusoidal background due to electric field variations induced by frequent tiny variations of the Earth’s magnetic field of extraterrestrial origin. Examples of applying DFA to such time series are presented. Upon approaching a major earthquake, however, the feature of the electrical records markedly change, because upon the appearance of the precursory SES activity a large number of dichotomous electric pulses superimpose on the pseudosinusoidal background thus leading to significantly different results of DFA the description of which reveals the existence of three scaling exponents (“non-uniform” scaling). A similar behavior is found when analyzing magnetic records, since magnetic field variations accompany an SES activity.

I. INTRODUCTION

Xu et al.¹ reported that anomalous variations of the geomagnetic field have been observed prior to the M_w 9.0 Tohoku earthquake (EQ) that occurred in Japan on 11 March 2011. In

particular, the original records of the geomagnetic field at the Esashi (ESA) station located at about 135 km from the epicenter exhibited anomalous behavior for about 10 days (4 to 14 January 2011) mainly in the vertical component approximately 2 months before the M_w 9.0 earthquake. The findings of Xu et al.¹ were found² to be in full accord with results published independently^{3,4} on the basis of the analysis of seismicity of Japan in a new time domain -termed natural time⁵- which reveals some dynamic features hidden⁶ in the time series of complex systems⁷. Natural time analysis has been applied to diverse fields including seismicity (e.g., the correlation properties between consecutive earthquake magnitudes^{8,9} and how they are affected when a major event is impending¹⁰), heart rate variability¹¹ and systems exhibiting self-organized criticality¹². The results of Refs. 3,4 could be summarized as follows:

First, Varotsos et al.³ identified that the fluctuations of the order parameter of seismicity defined in natural time¹³ exhibited a clearly detectable minimum approximately at the time of the initiation of the pronounced Seismic Electric Signals (SES) activity observed by Uyeda et al.¹⁴ almost two months before the onset of the volcanic-seismic swarm activity in 2000 in the Izu Island region, Japan. SES are low frequency (≤ 1 Hz) changes of the electric field of the earth that have been found in Greece^{5,15,16} and Japan¹⁷ to precede earthquakes with lead times ranging from several hours to a few months. They are generated by means of the following mechanism¹⁸: In the focal area there exist ionic constituents in which the presence of aliovalent impurities produce extrinsic point defects¹⁹ which are attracted by the impurities thus forming electric dipoles²⁰. The relaxation time of these dipoles depend on temperature and pressure⁷. Before an EQ the stress σ gradually increases, which may reflect a decrease of the relaxation time, thus it may reach a *critical* value when $\sigma = \sigma_{cr}$. This results in a cooperative orientation of the electric dipoles leading to an emission of a transient electric signal which constitutes an SES. A number of such signals within a short time is called¹⁵ SES activity and the natural time analysis of the subsequent seismicity enables the identification^{21,22} of the time-window of the forthcoming major EQ.

Second, Sarlis et al.⁴ proceeded to the analysis of the Japan seismic catalog in natural time from 1 January 1984 to 11 March 2011 and demonstrated that the fluctuations of the order parameter of seismicity showed distinct minima a few months before all the shallow earthquakes of magnitude 7.6 or larger during this 27 year period in Japanese area. Among these minima, the deepest one was observed before the M_w 9.0 Tohoku earthquake on ~ 5

January 2011. This fact, in view of the aforementioned findings of Varotsos et al.³, reflects that a strong SES activity should have been initiated on the same date, i.e., on ~ 5 January 2011. The SES activities are accompanied by magnetic field variations, which are clearly detectable at distances of the order of ~ 100 km for EQs of magnitude 6.5 or larger²³, appearing mainly²⁴ in the Z component, e.g., see Ref. 25.

In an independent study Rong et al.²⁶ analyzed the daily scaling properties of geomagnetic time series from 1 January 2010 to 30 April 2011 recorded at three stations near the epicenter of the M_w 9.0 Tohoku EQ. By employing the detrended fluctuation analysis (DFA) -see below-, deviations from uniform power-law scaling were identified and quantified using a scaling index. They suggested²⁶ that a significant increase of “non-uniform” scaling index appeared well before the Tohoku EQ and concluded that the scaling properties of the local nonlinear system are possibly affected by the Tohoku EQ. It is the scope of this short paper to indicate that this precursory increase of the “non-uniform” scaling behavior in the magnetic field data can find a reasonable explanation on the basis of the aforementioned proposal², i.e., that the anomalous magnetic field variations are the ones which accompany the SES activity initiated around 5 January 2011 mentioned above.

II. DETRENDED FLUCTUATION ANALYSIS. MONOFRACTALS AND MULTIFRACTALS BACKGROUND

The signals emitted from complex systems exhibit fluctuations over multiple scales which are characterized by absence of dynamic scale, i.e., scale-invariant behavior²⁷. These signals are typically non-stationary and their reliable analysis should not be carried out by traditional methods, e.g., power-spectrum and auto-correlation analysis²⁸⁻³⁰. On the other hand Detrended Fluctuation Analysis (DFA)^{31,32} has been established as a robust method suitable for detecting long-range power-law correlations embedded in non-stationary signals and has been applied with successful results to diverse fields where scale-invariant behavior emerges, such as DNA³³, heart dynamics^{34,35}, circadian rhythms³⁶, meteorology³⁷ and climate temperature fluctuations³⁸, economics³⁹ as well as in SES activities⁴⁰⁻⁴² along with their relevant^{16,23,24,43} magnetic field variations⁴².

Monofractal signals are homogeneous in the sense that they have the same scaling properties, characterized locally by a single singularity exponent h_0 , throughout the signal. Thus,

monofractal signals can be indexed by a single global exponent, e.g., the Hurst²⁸ exponent $H \equiv h_0$, which suggests that they are stationary from viewpoint of their local scaling properties (see Refs. 34,35 and references therein). Since the traditional DFA can measure only one exponent, this method is more suitable for the investigation of monofractal signals (this is alternatively termed as a case of a “uniform” scaling). In this case the root mean square variability of the detrended process in DFA varies with the scale s as $F(s) \propto s^\alpha$ (see also below). In some cases, however, the records cannot be accounted for by a single scaling exponent, i.e., they do not exhibit a simple monofractal behavior. In general, if a number of scaling exponents is required for a full description of the scaling behavior, a multifractal analysis must be applied. A reliable multifractal analysis can be performed by the Multifractal Detrended Fluctuation Analysis, MF-DFA⁴⁴ or by the wavelet transform (e.g., see Refs. 34,45).

A brief description of DFA is as follows. We first calculate the ‘profile’:

$$y(n) = \sum_{i=1}^n (x_i - \bar{x}) \quad (1)$$

of a time series $\{x_i\}$, $i = 1, 2, \dots, N$ with mean \bar{x} :

$$\bar{x} = \frac{1}{N} \sum_{i=1}^N x_i \quad (2)$$

where N is the length of the signal.

Second, the profile $y(n)$ is divided into $N_s \equiv [N/s]$ non overlapping segments of equal length (“scale”) s . Third, we estimate a (piecewise) polynomial trend $y_s^{(l)}(n)$ within each segment by least-squares fitting, i.e., $y_s^{(l)}(n)$ consists of concatenated polynomials of order l which are calculated separately for each of the segments. The degree of the polynomial can be varied in order to eliminate linear ($l = 1$), quadratic ($l = 2$), or higher order trends⁴⁶ of the profile function. DFA is named after the order of the fitting polynomial, i.e., DFA-1 if $l = 1$, DFA-2 if $l = 2, \dots$. Note that, due to the integration procedure in the first step, DFA- l removes polynomial trends of order $l - 1$ in the original signal $\{x_i\}$. Fourth, the detrended profile function $\tilde{y}_s(n)$ on scale s is determined by

$$\tilde{y}_s(n) = y(n) - y_s^{(l)}(n) \quad (3)$$

which, in other words, means that the profile $y(n)$ is detrended by subtracting the local

trend in each segment. Fifth, the variance of $\tilde{y}_s(n)$ yields the fluctuation function on scale s

$$F(s) = \sqrt{\frac{1}{N} \sum_{n=1}^N [\tilde{y}_s(n)]^2} \quad (4)$$

Sixth, the above computation is repeated for a broad number of scales s to provide a relationship between $F(s)$ and s . A power law relation between $F(s)$ and s , i.e.,

$$F(s) \propto s^\alpha \quad (5)$$

indicates the presence of scale-invariant (fractal) behavior embedded in the fluctuations of the signal. The fluctuations can be characterized by the scaling exponent α , a self-similarity parameter: If $\alpha = 0.5$, there are no correlations in the data and the signal is uncorrelated (white noise); the case $\alpha < 0.5$ corresponds to anti-correlations, meaning that large values are most likely to be followed by small values and vice versa. If $\alpha > 0.5$, there are long range correlations, which are stronger⁴⁷ for higher α . Note that $\alpha > 1$ indicates a non-stationary local average of the data and the value $\alpha = 1.5$ indicates Brownian motion (integrated white noise).

Compared to DFA in the MF-DFA the following additional two steps should be made:

First, we average over all segments to obtain the q -th order fluctuation function $F_q(s)$:

$$F_q(s) \equiv \left\{ \frac{1}{N_s} \sum_{\nu=1}^{N_s} [F^2(s, \nu)]^{\frac{q}{2}} \right\}^{\frac{1}{q}} \quad (6)$$

where

$$F^2(s, \nu) = \frac{1}{s} \sum_{n=(\nu-1)s+1}^{\nu s} \tilde{y}_s(n)^2, \quad (7)$$

and the index variable q can take any real value except zero. This is repeated for several scales s .

Second, we determine the scaling behavior of the fluctuation functions by analyzing log-log plots $F_q(s)$ versus s for each value of q . For long-range power-law correlated series, $F_q(s)$ varies as

$$F_q(s) \propto s^{h(q)}, \quad (8)$$

where the function $h(q)$ is called generalized Hurst exponent. For stationary time series the aforementioned Hurst exponent H is identical to $h(2)$,

$$h(2) = H. \quad (9)$$

III. RESULTS OF APPLYING DFA TO SES ACTIVITIES AND THEIR ASSOCIATED MAGNETIC FIELD VARIATIONS

When trying to identify anomalous electric field variations, and hence SES activities, our electrical records are contaminated by noise mainly due to the following two origins: First, artificial noise (AN) comprising electric signals emitted from man-made sources located close to the measuring station. AN may look to be similar to SES activities. Second, electric variations induced by small changes of the Earth's magnetic field (magnetotelluric variations, MT) of extraterrestrial origin are practically continuously superimposed on our records. MT variations are easily recognized when a network of measuring stations is operating since they appear almost simultaneously at the records at all measuring sites. On the other hand, the recognition of AN is more difficult and can be achieved by means of DFA and MF-DFA upon employing also natural time analysis as follows:

When DFA is applied to the original time series of the SES activities and AN, it was found⁴⁰ that both types of signals lead to a slope at short time scales (i.e., $\Delta t \leq 30s$) lying in the range $\alpha=1.1-1.4$, while for longer time scales the range $\alpha=0.8-1.0$ was determined without, however, any safe classification between SES activities and AN. On the other hand, when employing natural time, DFA enables the distinction between SES activities and artificial noises: for the SES activities the α -values lie approximately in the range 0.9 - 1.0, while for the AN the α -values are markedly smaller, i.e., $\alpha=0.65-0.8$. This reflects that the SES activities exhibit infinitely ranged temporal correlations, which is not the case for the AN. The fact that $\alpha \approx 1$ has been also verified⁴² for the magnetic field variations accompanying the SES activities.

MF-DFA was also applied⁴⁰ to the time series of SES activities and AN. This multifractal analysis, when carried out in the conventional time frame, did not lead to any distinction between these two types of signals. On the other hand, if the analysis is made in natural time, a distinction becomes possible⁴⁰. In particular, when the MF-DFA is applied in natural time reveals that the $h(q)$ curves for the SES activities lie systematically higher than those in the case of "artificial" noises. For example, for $q = 2$ the $h(2)$ values for the SES activities lie close to unity. A similar behavior is expected to hold also for the magnetic field variations associated with the SES activities. On the other hand, the $h(2)$ values for AN scatter⁴¹ approximately in the range 0.65-0.8 (see also Subsection 4.5.3 of Ref.7).

Multifractal analysis of various SES activities in Greece has been also performed⁴¹ by using the wavelet transform instead of MF-DFA.

In view of the above, it is thereafter taken as granted that AN are distinguished from SES activities. Hence, in what remains we focus on the study of the case of electrical records when MT are present together with the SES activities by employing DFA. To facilitate our study we first start from an example in which SES activities are absent and hence only MT are superimposed on our records. Such a recent example is depicted in Fig.1(a) that has been recorded on 7 December 2013 at a station located close to Patras city in Western Greece. The red color corresponds to the record as received of ~ 14 hour duration taken with sampling frequency 1 sample/sec while in the blue one in each point we have plotted the average values of the previous 60 measurements (in a similar fashion as Rong et al.²⁶ did). The DFA plots resulting from the analysis of both these curves are shown in Fig.1(b) by using the corresponding color. An inspection of this figure reveals that in both cases there exists a single crossover (marked with an arrow) at the time scale ~ 160 s. At the part of the DFA plot corresponding to shorter scales we deduce an α -exponent around $\alpha \sim 1.8$ for the former curve and $\alpha \sim 2.0$ for the latter while at the larger scales the slope of this log-log plot for both curves leads to a smaller exponent, i.e., $\alpha \sim 1.2$. Our finding that in the shorter scales the α -exponent is $\alpha \sim 2.0$ agrees with the results of Fig. 5 of Hu et al.⁴⁸ when they studied pseudosinusoidal functions with different amplitudes and periods.

We now turn to a second example in which, beyond MT variations, SES activities are present in our electrical records. This, in other words, means that we have considered a time period close to the occurrence of an impending strong EQ. Such an example is depicted in Fig.2(a) in which the red color presents the original recording of an SES activity collected at a station located close to Pírgos town in Western Greece from 29 February to 2 March 2008. This SES activity, which preceded the disastrous $M_w 6.5$ EQ that occurred with an epicenter at $38.0^\circ\text{N } 21.5^\circ\text{E}$ lying between Pírgos and Patras only a few tens of km away from the measuring site, is superimposed on a pseudosinusoidal background arising from MT variations. The procedure through which this pseudosinusoidal background can be subtracted should also employ natural time analysis and has been described in detail by Varotsos et al.⁴². After subtracting it, we find the channel shown in green which is the true SES activity of obvious dichotomous nature (this is the lowest channel “e” of Fig. 4 of Ref. 42). We now apply DFA to an excerpt of the original record -shaded in Fig.2(a)- of several

hours duration (~ 8.3 h) which contains a portion of the SES activity. This excerpt is shown in expanded time scale in Fig.2(b). The DFA plot resulting from this excerpt is depicted in Fig.3 and comprises three parts shown in red, blue and green. Two cross-overs (marked with arrows) are observed at the time scales ~ 32 s and ~ 320 s. The parts corresponding to the shortest and the largest scales (i.e., the ones shown in red and green, respectively) lead to a more or less similar slope, i.e., $\alpha \sim 1.1$, which is very close to unity, while the intermediate part result in $\alpha \sim 1.3$. In other words, when comparing the DFA plots depicted in Fig. 1(b) and Fig. 3 exhibiting one cross-over and two cross-overs respectively, which could be interpreted it as showing an increase of the “non-uniform” scaling behavior upon analyzing an excerpt of the original record that contains MT variations (pseudosinusoidal) together with a portion of the SES activity (dichotomous nature, see also below). By the same token, a similar behavior should be also found when analyzing the magnetic field variations -instead of the electric field ones- accompanying an SES activity. For the sake of comparison, we also plot (in black) in Fig.3 the results deduced from the DFA analysis of the SES activity alone, i.e., the signal of dichotomous nature plotted in green in Fig.2(a). This reveals an almost linear $\log F(s)$ vs $\log s$ plot with an exponent $\alpha \approx 1$ which remains practically the same irrespective if we apply DFA-1, DFA-2 or DFA-3, see Ref. 42.

To examine what happens on the “non-uniform” scaling behavior when the amplitude of the SES activity increases we work as follows:

The extent to which the “non-uniform” scaling behavior depends on the amplitude E of the SES activity can be visualized in Fig. 4. In particular, the upper panel of Fig. 4 depicts the DFA plot of the 8.3 hour excerpt -shaded in Fig. 2 (a) and shown in expanded time scale in 2 (b)- containing a portion of the SES activity that preceded the aforementioned $M_w 6.5$ EQ in Greece in 2008. Based on this portion and by making use of the scaling relation $\log E = 0.33M + \text{const}$ that interconnects the SES amplitude with the magnitude M of the subsequent EQ, we constructed the corresponding portions that would appear before EQs of stronger magnitude and analyzed then by DFA. Specifically, the other panels b, c, d of Fig. 4 refer to the DFA plots resulting from the analysis of SES activities of larger amplitude that correspond to stronger EQs of magnitude $M = 7.5, 8.5$ and 9.0 , respectively. An inspection of these plots reveals that a systematic change emerged, i.e., the exponent α at the largest scales decreases upon increasing the EQ magnitude; the α values, as shown in Fig. 4, are $\alpha = 0.86, 0.50, 0.30$ and 0.26 for $M + w = 6.5, 7.5, 8.5$ and 9.0 , respectively.

In other words, the “non-uniform” scaling seems to be more evident when analyzing SES activities of dichotomous nature that precede EQs of larger magnitude.

IV. SUMMARY AND CONCLUSIONS

Here, we showed that the DFA plot resulting from a time-series of a regular electrical record in which only MT variations are superimposed, it exhibits a single cross-over. On the other hand, when our analysis refers to a period before a major EQ and hence the electrical record contains also an excerpt of an SES activity, the DFA plot reveals an evident increase of the “non-uniform” scaling behavior since two cross-overs now emerge. This should also hold for the corresponding magnetic field records, i.e., when an excerpt of the magnetic field variations accompanying an SES activity is contained in the data analyzed. This explains the increase of the “non-uniform” scaling behavior observed by Rong et al.²⁶, since -as we suggested in Ref. 2- the anomalous magnetic field variations identified by Xu et al.¹ well before the 2011 M_w 9.0 Tohoku EQ might be the ones that accompany a strong SES activity on ~5 January 2011.

* Electronic address: eskordas@phys.uoa.gr

¹ G. Xu, P. Han, Q. Huang, K. Hattori, F. Febriani, and H. Yamaguchi, *Journal of Asian Earth Sciences* **77**, 59 (2013), ISSN 1367-9120.

² E. S. Skordas and N. V. Sarlis, *Journal of Asian Earth Sciences* **80**, 161 (2014).

³ P. A. Varotsos, N. V. Sarlis, E. S. Skordas, and M. S. Lazaridou, *Tectonophysics* **589**, 116 (2013).

⁴ N. V. Sarlis, E. S. Skordas, P. A. Varotsos, T. Nagao, M. Kamogawa, H. Tanaka, and S. Uyeda, *Proceedings of the National Academy of Sciences* **110**, 13734 (2013).

⁵ P. A. Varotsos, N. V. Sarlis, and E. S. Skordas, *Phys. Rev. E* **66**, 011902 (2002).

⁶ S. Abe, N. V. Sarlis, E. S. Skordas, H. K. Tanaka, and P. A. Varotsos, *Phys. Rev. Lett.* **94**, 170601 (2005).

⁷ P. A. Varotsos, N. V. Sarlis, and E. S. Skordas, *Natural Time Analysis: The new view of time. Precursory Seismic Electric Signals, Earthquakes and other Complex Time-Series* (Springer-

- Verlag, Berlin Heidelberg, 2011).
- ⁸ P. V. Varotsos, N. V. Sarlis, E. S. Skordas, and H. K. Tanaka, Proc. Japan Acad., Ser. B **80**, 429 (2004).
 - ⁹ P. A. Varotsos, N. V. Sarlis, E. S. Skordas, H. K. Tanaka, and M. S. Lazaridou, Phys. Rev. E **74**, 021123 (2006).
 - ¹⁰ N. Sarlis, E. Skordas, and P. Varotsos, Tectonophysics **513**, 49 (2011).
 - ¹¹ N. V. Sarlis, E. S. Skordas, and P. A. Varotsos, EPL **87**, 18003 (2009).
 - ¹² N. Sarlis, E. Skordas, and P. Varotsos, EPL **96**, 28006 (2011).
 - ¹³ P. A. Varotsos, N. V. Sarlis, H. K. Tanaka, and E. S. Skordas, Phys. Rev. E **72**, 041103 (2005).
 - ¹⁴ S. Uyeda, M. Kamogawa, and H. Tanaka, J. Geophys. Res. **114**, B02310 (2009).
 - ¹⁵ P. Varotsos, N. Sarlis, and M. Lazaridou, Acta Geophysica Polonica **48**, 141 (2000).
 - ¹⁶ P. Varotsos, N. Sarlis, and E. Skordas, EPL (Europhysics Letters) **99**, 59001 (2012).
 - ¹⁷ S. Uyeda, T. Nagao, Y. Orihara, T. Yamaguchi, and I. Takahashi, Proc. Natl. Acad. Sci. USA **97**, 4561 (2000).
 - ¹⁸ P. Varotsos and K. Alexopoulos, *Thermodynamics of Point Defects and their Relation with Bulk Properties* (North Holland, Amsterdam, 1986).
 - ¹⁹ P. Varotsos and K. Alexopoulos, J. Phys. Chem. Sol. **41**, 443 (1980).
 - ²⁰ P. Varotsos and K. Alexopoulos, J. Phys. Chem. Sol. **42**, 409 (1981).
 - ²¹ N. V. Sarlis, E. S. Skordas, M. S. Lazaridou, and P. A. Varotsos, Proc. Japan Acad., Ser. B **84**, 331 (2008).
 - ²² P. A. Varotsos, N. V. Sarlis, and E. S. Skordas, Practica of Athens Academy **76**, 294 (2001).
 - ²³ P. V. Varotsos, N. V. Sarlis, and E. S. Skordas, Phys. Rev. Lett. **91**, 148501 (2003).
 - ²⁴ N. Sarlis and P. Varotsos, J. Geodynamics **33**, 463 (2002).
 - ²⁵ P. Varotsos, N. Sarlis, K. Eftaxias, M. Lazaridou, N. Bogris, J. Makris, A. Abdulla, and P. Kapiris, Phys. Chem. Earth (A) **24**, 115 (1999).
 - ²⁶ Y.-M. Rong, Q. Wang, X. Ding, and Q.-H. Huang, Chinese Journal of Geophysics **55**, 3709 (2012).
 - ²⁷ H. E. Stanley, Nature **378**, 554 (1995).
 - ²⁸ H. E. Hurst, Trans. Am. Soc. Civ. Eng. **116**, 770 (1951).
 - ²⁹ B. B. Mandelbrot and J. R. Wallis, Water Resources Research **5**, 321 (1969).
 - ³⁰ R. L. Stratonovich, *Topics in the Theory of Random Noise, vol.I* (Gordon and Breach, New

- York, 1981).
- ³¹ C.-K. Peng, S. V. Buldyrev, S. Havlin, M. Simons, H. E. Stanley, and A. L. Goldberger, *Phys. Rev. E* **49**, 1685 (1994).
 - ³² M. S. Taqqu, V. Teverovsky, and W. Willinger, *Fractals* **3**, 785 (1995).
 - ³³ C.-K. Peng, S. V. Buldyrev, A. L. Goldberger, S. Havlin, M. Simons, and H. E. Stanley, *Phys. Rev. E* **47**, 3730 (1993).
 - ³⁴ P. C. Ivanov, M. G. Rosenblum, C.-K. Peng, J. Mietus, S. Havlin, H. E. Stanley, and A. L. Goldberger, *Nature* **399**, 461 (1999).
 - ³⁵ P. C. Ivanov, L. A. N. Amaral, A. L. Goldberger, S. Halvin, M. G. Rosenblum, H. E. Stanley, and Z. R. Struzik, *CHAOS* **11**, 641 (2001).
 - ³⁶ K. Hu, P. C. Ivanov, Z. Chen, M. F. Hilton, H. E. Stanley, and S. A. Shea, *Physica A* **337**, 307 (2004).
 - ³⁷ K. Ivanova and M. Ausloos, *Physica A* **274**, 349 (1999).
 - ³⁸ E. Koscielny-Bunde, A. Bunde, S. Havlin, H. E. Roman, Y. Goldreich, and H.-J. Schellnhuber, *Phys. Rev. Lett.* **81**, 729 (1998).
 - ³⁹ N. Vandewalle and M. Ausloos, *Physica A* **246**, 454 (1997).
 - ⁴⁰ P. A. Varotsos, N. V. Sarlis, and E. S. Skordas, *Phys. Rev. E* **67**, 021109 (2003).
 - ⁴¹ P. A. Varotsos, N. V. Sarlis, and E. S. Skordas, *Phys. Rev. E* **68**, 031106 (2003).
 - ⁴² P. A. Varotsos, N. V. Sarlis, and E. S. Skordas, *CHAOS* **19**, 023114 (2009).
 - ⁴³ P. Varotsos, N. Sarlis, and E. Skordas, *Proc. Jpn. Acad., Ser. B* **77**, 93 (2001).
 - ⁴⁴ J. Kantelhardt, S. A. Zschiegner, E. Koscielny-Bunde, A. Bunde, S. Havlin, and H. E. Stanley, *Physica A* **316**, 87 (2002).
 - ⁴⁵ J. F. Muzy, E. Bacry, and A. Arneodo, *Int. J. Bifurcation Chaos* **4**, 245 (1994).
 - ⁴⁶ A. Bunde, S. Havlin, J. W. Kantelhardt, T. Penzel, J.-H. Peter, and K. Voigt, *Phys. Rev. Lett.* **85**, 3736 (2000).
 - ⁴⁷ A. Bashan, R. Bartsch, J. W. Kantelhardt, and S. Havlin, *Physica A* **387**, 5080 (2008).
 - ⁴⁸ K. Hu, P. C. Ivanov, Z. Chen, P. Carpena, and H. E. Stanley, *Phys. Rev. E* **64**, 011114 (2001).

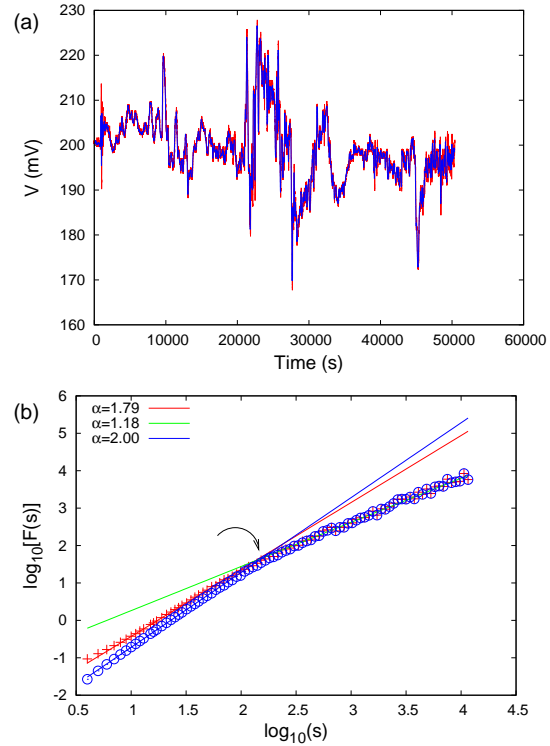


FIG. 1: (color online) (a) An almost 14h excerpt of the electrical field records during which MT variations were also present on 7 December 2013 at a station located close to Patras city in Western Greece; red: as received when using a sampling frequency 1 sample/sec; blue: when plotting (at each point) the average value of its previous 60 measurements (b) the DFA-1 plots for the time series mentioned in (a) upon using the same colors. There exists a single cross-over indicated by the arrow.

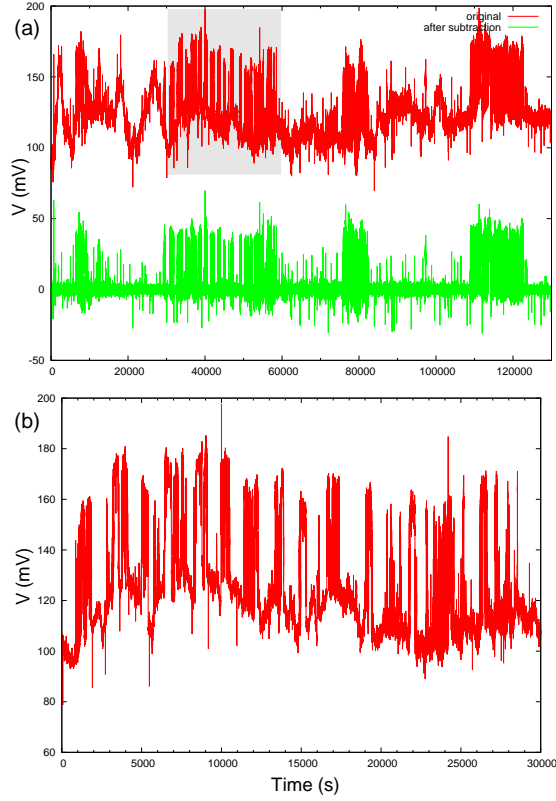


FIG. 2: (color online) (a) The red color represents the original record of the SES activity at a station close to Pirgos town in Western Greece, which lasted from 29 February to 2 March 2008. This SES activity was superimposed on a pseudosinusoidal background, due to MT variations, which are evident in the left part of the figure. After subtracting the MT background -by means of the procedure described in Ref. 42- the green signal of dichotomous nature remains which constitutes the true precursory signal, i.e., the SES activity. (b) An almost 8.3 h excerpt of the original record (shaded in (a)) is plotted here in expanded time scale.

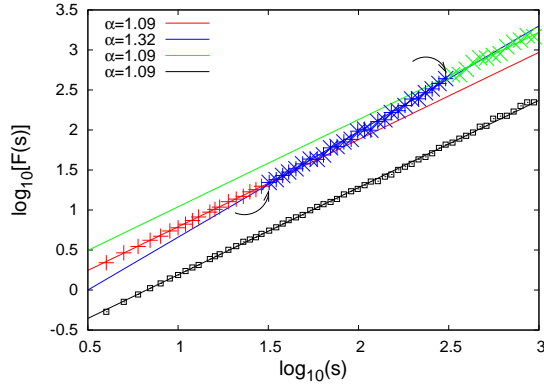


FIG. 3: (color online) The DFA plot resulting from the analysis of an excerpt -shaded in Fig. 2(a)- of the original time series of the SES activity plotted in red in Fig. 2(a) superimposed on MT variations. It comprises three parts -shown in red, blue and green- two of which, i.e., the ones corresponding to the shortest and the largest scales, are depicted in red and green, respectively. The two cross-overs observed are marked with arrows. For the sake of comparison, the plot in black depicts the results deduced from the DFA analysis (shifted vertically for the sake of clarity) when considering the SES activity alone, i.e., the signal of dichotomous nature plotted in green in Fig. 2(a)

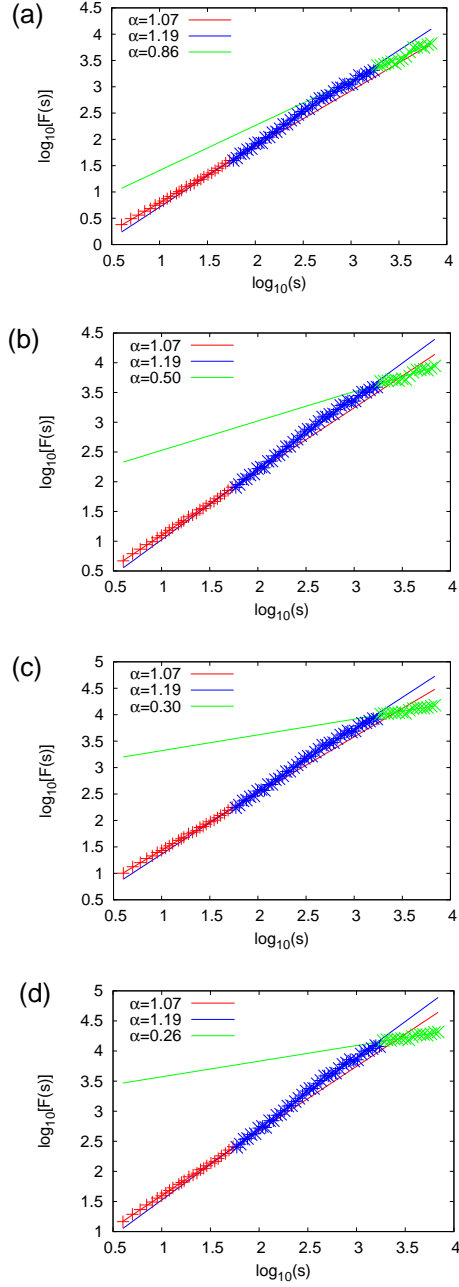


FIG. 4: (color online) The DFA plots resulting from the analyses of excerpts of SES activities that precede EQs of various magnitudes $M_w=6.5$ (a), 7.5 (b), 8.5 (c) and 9.0 (d) (see the text)